Supporting Information

Amidoximated Poly(Vinyl Imidazole)-Functionalized Molybdenum Disulfide Sheets for Efficient Sorption of Uranyl Tricarbonate Complex from Aqueous Solutions

Liang Shen [a], *Xiaoli Han* [a], *Jun Qian* [a], *Daoben Hua* [a,b*]

[a] School for Radiological and Interdisciplinary Sciences (RAD-X)& College of Chemistry, Chemical Engineering and Materials Science, Soochow University, Suzhou 215123, China

[b] Collaborative Innovation Center of Radiological Medicine of Jiangsu Higher Education Institutions, Suzhou 215123, China

Table of contents

1. Characterization methods

^{1}H nuclear magnetic resonance (^{1}H NMR) spectrum was recorded by Varian INVOA-400 instrument (400 MHz). The molecular weight of the polymer was determined using a Waters 1515 gel permeation chromatographer (GPC) with HR1, HR3, and HR4 column, equipped with refractive index detector and calibrated with PS standard samples with molecular weight range (100 – 500,000), DMF as the eluent at a flow rate of 1.0 mL/min and operated at 30 ℃. Transmission electron microscopy (TEM) images were filmed by a FEI Tecnai G20 electron microscope (accelerating voltage, 200 kV). X-ray photoelectron spectroscopy (XPS) was performed on ESCALAB 250 microprobe system with monochromatization of an exciting X-ray radiation. Malvern Zeta sizer (632.8 nm, He-Ne laser) was used to record the zeta potential and Z-average size distribution of the corresponding materials. Thermogravimetric analysis (TGA) was performed on TG/DTA 6300 in a N_2 flow. Powder X-ray diffraction (XRD) data were collected from 10° to 80° with a step of 0.02° and the time for data collection was 0.5 s on a Bruker D8 Advance diffractometer with Cu K_α radiation (λ=1.54056 Å) and a Lynxeye one-dimensional detector. Fourier transform infrared (FT-IR) spectra were performed with Varian-1000 spectrometer. Field-emitting scanning electron microscopy (SEM) images were taken by using a HITACHI S-570 microscope operated at an accelerating voltage of 15 kV. The concentrations of uranium(VI) were determined by thermo high resolution inductively coupled plasma mass spectrometer (ICP-MS, Element II). Elemental analysis (EA) was determined by ELEMENTAR CHNOS Elemental Analyzer.

2. *S*-1-dodecyl-*S′*-(*α*,*α′*-dimethyl-*α″*-acetic acid) trithiocarbonate (DDATC)

DDATC was prepared according to the reference[1]. Typically, 1-dodecanethiol (5.050 g, 0.250 mol), tricaprylylmethylammonium chloride (0.406 g, 0.001 mol), and acetone (12.020 g, 0.207 mol) were added in a round-bottomed flask at 10 °C under nitrogen atmosphere. Then sodium hydroxide solution (50%, 2.096 g, 0.026 mol) was added dropwise over 20 min. The reaction was stirred for additional 15 min before carbon disulfide (1.901 g, 0.025 mol) in acetone (2.522 g, 0.043 mol) was added over 20 min. Ten minutes later, chloroform (4.452 g, 0.037 mol) was added in one portion, followed by dropwise adding 50% sodium hydroxide solution (10.0 g, 0.125 mol) over 30 min. The mixture was stirred overnight. 37.5 mL ultrapure water was added, followed by 6.25 mL concentrated HCl to acidify the aqueous solution. Nitrogen was purged through the reactor with

continuous stirring to help evaporate off acetone. The solid was collected and then dissolved in 2-propanol. The 2-propanol solution was concentrated to dryness, and the resulting solid was re-crystallized from hexanes. The structure of DDATC was characterized by ^{1}H NMR spectrum (Figure S1). The characteristic peaks at 0.87-0.96 ppm and 1.62-1.80 ppm (–CH_3), 3.25-3.38 ppm (–S-CH_2-) and 1.20-1.55 ppm (-CH_2-) indicated the successful synthesis of DDATC.

3. Synthesis of PVIAO

PVIAO was synthesized according to the modified literature method[2]. PVI was first synthesized by RAFT polymerization, and the typical recipe was as follows: vinyl imidazole (2.0 g, 21.3 mmol), DDATC (0.146 g, 0.4 mmol), AIBN (0.033 g, 0.2 mmol) and 4.0 mL DMF were added in an ampoule. The contents were purged with argon for 30 min to eliminate the oxygen. Then, the ampoule was flame-sealed and placed in an oil bath at 70 °C. After 20 h, the ampoule was cooling to room temperature and opened, and the mixture was diluted with DMF (10 mL) and then precipitated in diethyl ether (150 mL) for three times. The obtained PVI was dried in vacuum at 40 °C until a constant weight. Then, the PVI (0.3 g, 0.05 mmol) was reacted with 4-bromobutyronitrile (2.590 g, 17.5 mmol) in DMF (10 mL) at 70 °C for 8 h. The mixture was finally precipitated in diethyl ether (150 mL). The product was collected by centrifugation and dried in a vacuum oven at 40 °C. The resultant polymer was then reacted with hydroxylamine (2.770 g, 40.0 mmol) in H_2O (10 mL) at 80 °C for 12 h to convert acrylonitrile group to amidoxime group. Finally the mixture was lyophilized to give PVIAO. The structure of PVIAO was characterized by ^{1}H NMR spectrum (Figure S2). The peak at δ=4.00-5.00 ppm is assigned for the protons of propyl group, and the peak for the protons of imidazolyl group is shifted from 6.80-7.50 ppm to 7.70-8.50 ppm and 10.10 ppm for PVIAO due to the positive charges, which suggested that PVIAO was successfully synthesized.

4. Preparation of MoS_2-sheets

MoS_2-sheets were prepared by exfoliation of lithium-intercalated MoS_2 powder in water according to the modified method.[3, 4] A typical procedure is described below: inside argon glove box, 1.0 g of MoS_2 powder was submerged in 100 mL of 1.6 mol/L *n*-butyllithium solution in hexane for 48 h. After filtrated, washed with hexane several times and dried, the mixture was removed from glove box. The intercalated MoS_2 compound was then suspended in 100 mL ultrapure water and sonicated for 1 h. Exfoliated material was then dialyzed against continuous water flow using MW

3500 cut-off dialysis bag. MoS_2-sheets were then collected immediately.

5. Sorption kinetics

Pseudo-first-order equation represents the relationship between sorption amount q_t and time t:

$$\log(q_e - q_t) = \log q_e - (\frac{k_1}{2.303}) \times t \qquad (1)$$

where q_e and k_1 (s^{-1}) are the sorption capacity of uranium(VI) at equilibrium time and pseudo-first-order kinetic constant, respectively. q_e and k_1 can be calculated by slope and intercept of the plot of log (q_e-q_t) agains t, respectively (Figure S6A).

Pseudo-second-order model is expressed as Equation (2):

$$\frac{t}{q_t} = \frac{1}{k_2 \times q_e^{\ 2}} + \frac{t}{q_e} \qquad (2)$$

where k_2 (g/mg/s) represents the rate constant of the pseudo-second order model, which can be calculated from the plot of t/q_t versus t (Figure S6B).

6. Sorption isotherm

Langmuir model represents monolayer sorption based on the hypothesis that all the sorption sites have equal affinity and that desorption at one site doesn't influence an adjacent site, which can be described as Equation (3):

$$\frac{C_e}{q_e} = \frac{1}{q_{max} b} + \frac{C_e}{q_{max}} \qquad (3)$$

where b (L/mg) is the Langmuir constant, which is related to the affinity of binding sites, and q_{max} (mg/g) is the maximum sorption capacity. They can be calculated from the linear plot of C_e/q_e against C_e (Figure S7A).

The Freundlich model can be applied for multilayer sorption and the sorption on heterogeneous surfaces, which can be described as Equation (4):

$$\log q_e = \log K_F + \frac{1}{n} \log C_e \qquad (4)$$

where K_F ($mol^{n-1/n}L^{1/n}/g$) and n are Freundlich constants related to sorption capacity and sorption intensity, respectively. Both can be calculated from the linear plot of log q_e versus log C_e, respectively (Figure S7B).

Table S1. Comparison of rate constant (k_2) of pseudo-second order model of MoS_2-PVIAO with the other sorbents.

Matrix	pH	k_2 (g/mg/s)	Reference
Fe_3O_4@SiO_2-AO	5.0	2.80×10^{-5}	[5]
nZVI/rGO	5.0	1.07×10^{-7}	[6]
TiZr22-700	3.8	2.94×10^{-5}	[7]
PANI/H-TNB composite	5.0	1.39×10^{-5}	[8]
Nanodiamond-double-armed ligand	4.5	1.14×10^{-3}	[9]
PP-g-PVIm$^+$Br$^-$	8.0	1.57×10^{-7}	[10]
Bifunctional polymeric microspheres	7.0	9.17×10^{-6}	[2]
PAO_{76}-*b*-PS_{12}	7.8	9.39×10^{-5}	[11]
MoS_2-PVIAO (10.0%)	8.0	1.50×10^{-2}	This work
MoS_2-PVIAO (17.1%)	8.0	5.00×10^{-3}	This work

Table S2. Elemental analysis of MoS_2-sheets and MoS_2-PVIAO (17.1%) before and after five cycles experiment using HCl as eluent.

	Element %		
	Nitrogen	Carbon	Hydrogen
MoS_2-sheets	0.00	0.29	0.28
MoS_2-PVIAO (before)	6.47	16.26	2.49
MoS_2-PVIAO (after)	5.27	15.41	2.78

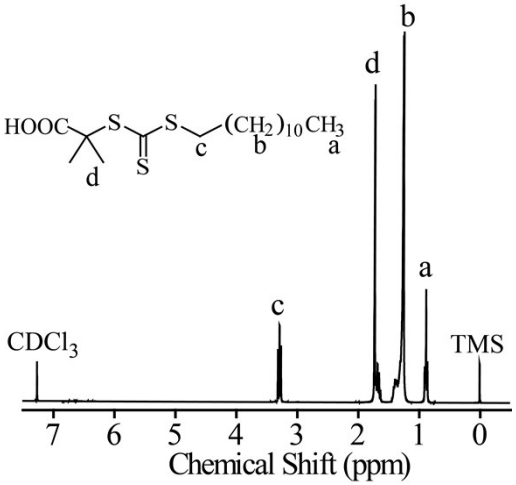

Figure S1. ^{1}H NMR spectrum (400M, $CDCl_3$) of DDATC.

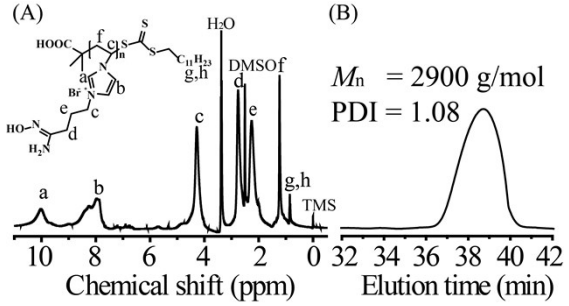

Figure S2. (A) ^{1}H NMR spectrum (400M, $CDCl_3$) of PVIAO; (B) GPC curve of PVIAO (M_n = 2900 g/mol, PDI = 1.08).

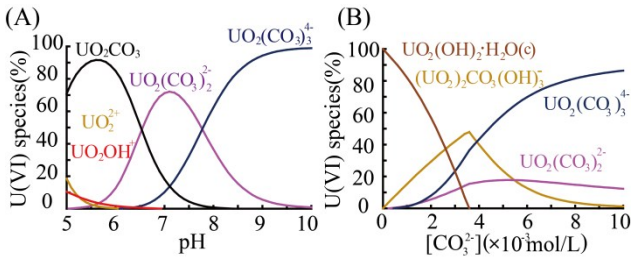

Figure S3. (A) Distribution of U(VI) species in aqueous solution with different pH, [U]= 1.4×10^{-8} mol/L; (B) Distribution of U(VI) species in aqueous solution with different CO_3^{2-} concentration, [U]= 3.3×10^{-4} mol/L and pH 8.0, which was simulated by Medusa program. There is no precipitation of uranium(VI) in the solution under the experimental condition in this study (i.e. pH 8.0, $[CO_3^{2-}]$ = 6.0×10^{-3} mol/L, and [U] = 3.3×10^{-4} mol/L).

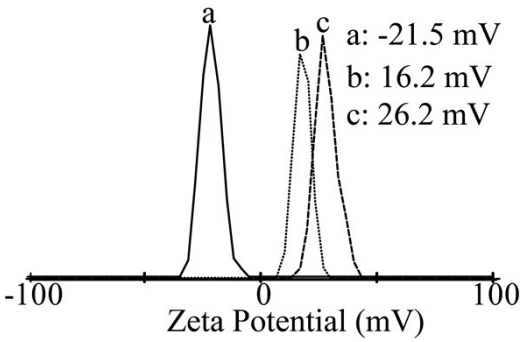

Figure S4. Zeta potential of (a) MoS_2-sheets, (b) MoS_2-PVIAO (10.0%), and (c) MoS_2-PVIAO (17.1%).

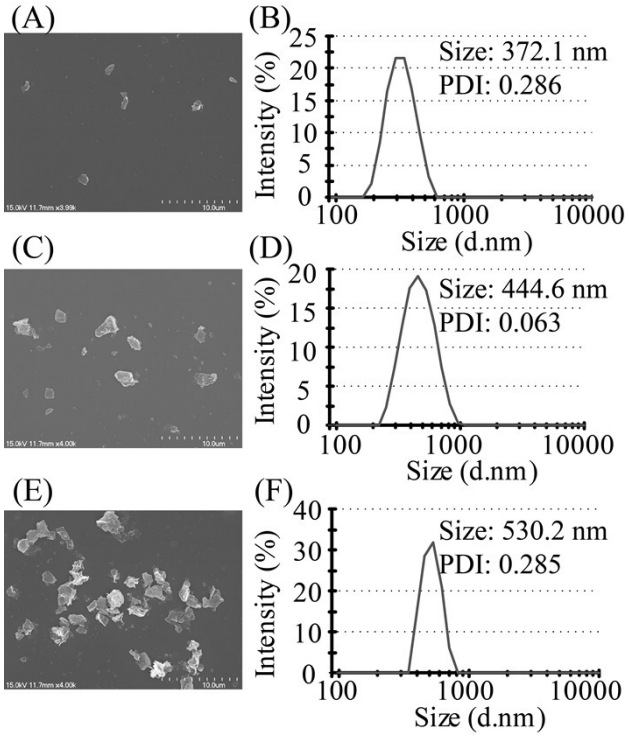

Figure S5. SEM images and particles size distributions of different concentration of MoS_2-PVIAO (17.1%) dispersed in water: (A, B) 0.08 g/L, (C, D) 0.16 g/L, (E, F) 0.32 g/L.

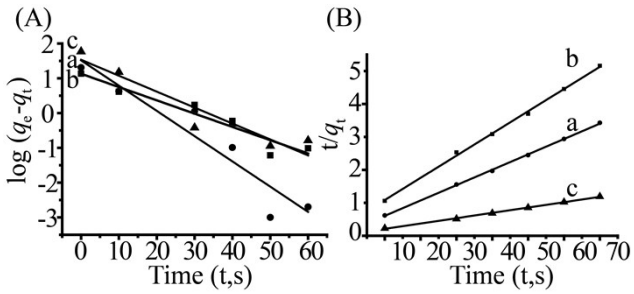

Figure S6. (A) Pseudo-first order kinetics and (B) pseudo-second order kinetics for the sorption of uranium(VI) with different sorbents: (a) MoS_2-sheets, (b) MoS_2-PVIAO (10.0%), (c) MoS_2-PVIAO (17.1%).

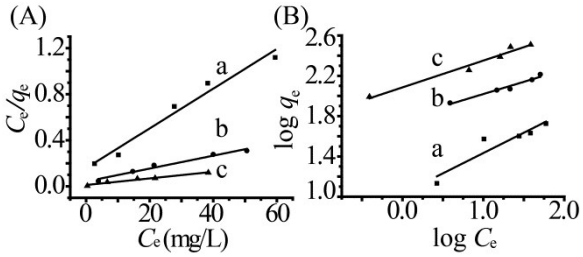

Figure S7. (A) Langmuir sorption isotherm plots and (B) Freundlich sorption isotherm plots for the sorption of uranium(VI) with different sorbents: (a) MoS_2-sheets, (b) MoS_2-PVIAO (17.1%) and (c)MoS_2-PVIAO (53.7%).

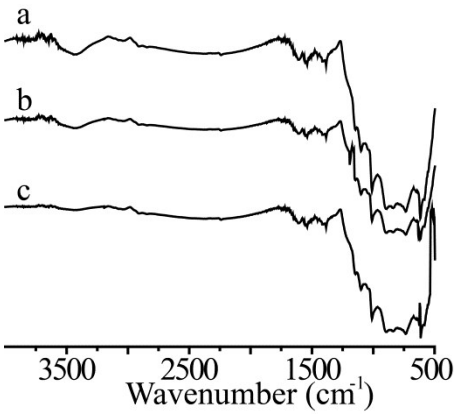

Figure S8. FT-IR spectra of (a) MoS_2-PVIAO (17.1%), (b) MoS_2-PVIAO (17.1%) after five cycles eluting with 0.1 mol/L HCl solution and (c) MoS_2-PVIAO (17.1%) after five cycles eluting with 1.0 mol/L $NaHCO_3$ solution.

References

1. J. T. Lai, A. Debby Filla and R. Shea, *Macromolecules*, 2002, **35**, 6754-6756.
2. Y. Wei, J. Qian, L. Huang and D. Hua, *RSC Adv.*, 2015, **5**, 64286-64292.
3. S. S. Chou, M. De, J. Kim, S. Byun, C. Dykstra, J. Yu, J. X. Huang and V. P. Dravid, *J. Am. Chem. Soc.*, 2013, **135**, 4584-4587.
4. K. Mao, Z. T. Wu, Y. R. Chen, X. D. Zhou, A. G. Shen and J. M. Hu, *Talanta*, 2015, **132**, 658-663.
5. Y. G. Zhao, J. X. Li, L. P. Zhao, S. W. Zhang, Y. S. Huang, X. L. Wu and X. K. Wang, *Chem. Eng. J.*, 2014, **235**, 275-283.
6. Y. B. Sun, C. C. Ding, W. C. Cheng and X. K. Wang, *J. Hazard. Mater.*, 2014, **280**, 399-408.
7. M. C. Kimling, N. Scales, T. L. Hanley and R. A. Caruso, *Environ. Sci. Technol.*, 2012, **46**, 7913-7920.
8. Y. Liu, Y. Y. Yang, L. Chen, H. S. Zhu, Y. H. Dong, N. S. Alharbi, A. Alsaedi and J. Hu, *RSC Adv.*, 2016, **6**, 56139-56148.
9. X. S. Zhao, S. Zhang, C. Y. Bai, B. Li, Y. Li, L. Wang, R. Wen, M. C. Zhang, L. J. Ma and S. J. Li, *J. Colloid Interface Sci.*, 2016, **469**, 109-119.
10. Z. H. Zeng, Y. Q. Wei, L. Shen and D. B. Hua, *Ind. Eng. Chem. Res.*, 2015, **54**, 8699-8705.
11. L. X. Zhang, L. Huang, Z. H. Zeng, J. Qian and D. B. Hua, *Phys. Chem. Chem. Phys.*, 2016, **18**, 13026-13032.